PAPER

Scaling behavior and morphology evolution of $CH_3NH_3PbI_3$ perovskite thin films grown by thermal evaporation

Materials Research Express

PAPER

Scaling behavior and morphology evolution of $CH_3NH_3PbI_3$ perovskite thin films grown by thermal evaporation

RECEIVED
13 April 2017

REVISED
8 June 2017

ACCEPTED FOR PUBLICATION
14 June 2017

PUBLISHED
21 July 2017

Yunyan Liu[1], Tong Zhou[1], Meiling Sun[1], Dong Zhao[1], Qinqin Wei[1], Yan Sun[1], Rendong Wang[1], Fangming Jin[2], Quanlin Niu[1] and Zisheng Su[2]

[1] School of Science, Shandong University of Technology, Zibo, Shandong 255049, People's Republic of China
[2] State Key Laboratory of Luminescence and Applications, Changchun Institute of Optics, Fine Mechanics and Physics, Chinese Academy of Sciences, Changchun 130033, People's Republic of China

E-mail: suzs@ciomp.ac.cn **and** niuql00@sdut.edu.cn

Keywords: perovskite, thin films, morphology evolution, thermal evaporation, growth mechanism

Abstract

The growth dynamics of $CH_3NH_3PbI_3$ ($MAPbI_3$) perovskite thin films, deposited by thermal evaporation, has been investigated by atomic force microscope and height–height correlation function analysis. The unstable scaling behavior of initial perovskite films exhibiting the growth of islands, resulting in rougher film formation has been observed. After the formation of continuous film, the roughening has been characterized by analyzing the scaling exponent $\alpha \sim 0.70$, growth exponent $\beta = 0.79 \pm 0.057$, $1/z = 0.78 \pm 0.038$, and 2D fast Fourier transform. Anomalous scaling behavior of the $MAPbI_3$ thin films and the formation of the rapid surface roughening are discovered. It is demonstrated that step-edge barrier induced mound growth may play the dominate role in the growth mechanism of $MAPbI_3$ thin films on Si substrates. Further, the growth behavior of $MAPbI_3$ film on ITO substrates is investigated as a comparison, and it reveals that the growth of MAPbI3 thin films is largely affected by the initial substrates underneath the growing films.

1. Introduction

Organometal halide perovskites have developed in a very fast speed owing to their optimum bandgap (1.2–2.3 eV), high absorption coefficient, long exciton diffusion length, and excellent charge transport property. Perovskites have found applications in many fields, ranging from photovoltaics to photodetector, to lasing and lighting [1–4]. As a promising candidate for future photovoltaic technology, the power conversion efficiency (PCE) of perovskite solar cells has rapidly increased from an initial value of 3.8%–22.1% in only 5 years [5, 6]. Although the perovskite solar cells and other perovskite optoelectronic devices have developed toward commercialization, device performance and stability are obsessed by problems associated with uniformity morphology, coverage and roughness of the perovskite films, and the formation dynamics understanding of the perovskite thin films is still challenging [7–9].

Great progress has been made in improving the morphology of the perovskite films by adjusting the solution concentration or interface layers, modifying the thermal treatment, or developing new deposition way [9–11]. Solution process via solution depositions and vacuum thermal evaporation [1, 4] are representative methods for fabricating perovskite based devices leading to exciting achievement. Among these methods, the vacuum thermal evaporation forms a perovskite film with the most homogeneous morphology, the highest coverage and superior stability, exhibiting outstanding performances of the corresponding devices. Detailed knowledge of growth dynamics of thin films is primary concern for better control of structural and morphology of thin films [9], however, to the best of our knowledge, understanding the growth mechanism of perovskite film for vacuum thermal evaporation has still been unknown.

Scaling theory has been developed to quantify the statistical properties of the morphology evolution of growth front, in hopes of getting some clues to complete understanding of the growth mechanism that enables one to achieve control over the growth at molecular level [12]. A large variety of discrete models and continuous equations have been established to relate physical growth mechanism and reveal a wealth of information about thin films growth. In this paper, we report the scaling behavior and related physical growth dynamics of $CH_3NH_3PbI_3$ ($MAPbI_3$) perovskite thin films on smooth Si substrates by vacuum thermal evaporation. By quantitatively

analyzing the scaling exponents α, β and $1/z$, elucidating the film morphology evolution with growing time, we find that the $MAPbI_3$ thin films on Si substrate display rapid rough of mound growth. For comparison, the dynamic behavior of $MAPbI_3$ thin films on rough ITO substrates has been discussed, and we aims to reveal the dependence of growth kinetics of $MAPbI_3$ thin films on surface properties of initial substrate most relevant for device applications.

2. Materials and methods

The $MAPbI_3$ perovskite thin films were fabricated by thermal evaporation on Si substrates. The substrates were routinely cleaned followed by UV-ozone treatment for 10 min. The background pressure of the vacuum chamber was 5×10^{-4} Pa, without breaking vacuum. The $MAPbI_3$ film was grown by thermal co-evaporating CH_3NH_3I and PbI_2. The purity of CH_3NH_3I and PbI_2 is 99% and the mass ratio of CH_3NH_3I and PbI_2 was 4:1. For this co-evaporation process, PbI_2 was first heated and then CH_3NH_3I. The shuttle mask was opened to ensure that the two precursors were evaporated simultaneously. The substrates were not intentionally heated during deposition and all the films were not post heat treated. The deposition rate was 0.5 Å s^{-1} for $MAPbI_3$ films, and the layer thickness was monitored *in situ* using oscillating quartz monitors. Thin film samples were grown with time of 130, 160, 200, 300, 500, and 600 s (corresponding to a thickness range of 6.5–30 nm). $MAPbI_3$ films were deposited on rough ITO coated glass substrates in the same deposition situation. The thickness and roughness of ITO substrate is 140 nm and 3.3 nm, respectively.

The surface topographies were imaged with a Bruker MultiMode 8 atomic force microscope (AFM) in tapping mode in air. The scanning area for AFM imaging was 3 μm $\times$ 3 μm and the resolution is 256 $\times$ 256. In order to get good statistical properties, repeated measurement of different regions of each $MAPbI_3$ film sample were carried out to obtain the averaged height–height correlation function $H(r, t)$, which was used as the height–height correlation function for the sample.

3. Theoretical basis

Quantitative study of roughness dynamics of the film surface can be obtained through the height–height correlation function $H(r, t)$. $H(r, t)$ is defined as a function of lateral position r and deposition time t by $H(r,t)=\langle[h(r,t) - h(0,t)]^2\rangle$, where $h(r, t)$ and $h(0, t)$ represent, respectively, the relative surface heights at lateral positions r and $r = 0$ at time t. Here the position $r = 0$ may be arbitrarily chosen for uniformly deposited thin film samples. The scaling hypothesis requires that the height–height correlation function in the scaling form as given by:

$$H(r,t) \propto \begin{cases} Cr^{2\alpha}, & r \ll \xi(t) \quad (a) \\ 2W^2(t), & r \gg \xi(t) \quad (b) \end{cases}. \tag{1}$$

Where roughness exponent α is used to describe the local randomly fluctuation of a surface. A larger value of α ($>$0.5) corresponds to a smooth short-range surface, while the small value of α ($<$0.5) corresponds to a more jagged local surface morphology. The interface width w (RMS), changes with growth time as $w_{(t)} \propto t^{\beta}$, where β is called the growth exponent. It describes how the vertical width of the surface scales with time. Correlation length ξ can be obtained through the cross-over region of $H(r, t)$. ξ provides a length scale which distinguishes the short-range and long-range behaviors of the rough surface, it is the distance within which the surface variations are correlated, and usually obeys the relationship of $\xi(t) \propto t^{1/z}$, where $1/z$ is called the dynamic exponent and it describes how the lateral length of surface scales with time. The relation between the three exponents $1/z = \beta/\alpha$ is required in truly self-affine growth, which is corresponding to the stationary growth. Scaling hypothesis does not hold if the relation between the scaling exponents is $\beta/\alpha = 1/z + \lambda$ ($\lambda \neq 0$) and λ is the steepening exponent [13].

4. Results and discussion

4.1. The morphology evolution and growth behavior of $MAPbI_3$ films deposited on Si substrates

Figure 1 shows the surface morphology and the corresponding 1D cross-section scans of surface profile of Si substrate and $MAPbI_3$ films deposited on Si measured by AFM. The films deposition time are 130, 200, 300, and 600 s, respectively. Figure 1(b) shows that isolated and coalesced islands distribute uniformly on the surface of the $MAPbI_3$ film with growth time of 130 s, which exhibits dramatically different morphology from that of smooth Si substrate (figure 1(a)). When films growth time is more than 200 s, the Si substrate surface is fully covered by $MAPbI_3$ thin film. The individual island is not observed anymore but growth of continuous film as shown in figures 1(c)–(e). 1D cross-section scans reveal that the surface height decreases with growth time at first. After the formation of continuous film, the surface fluctuation becomes bigger and bigger as the films thickness increases. The morphology evolution is a characteristic of coalescence and continuous film processes of Volmer–Weber-type

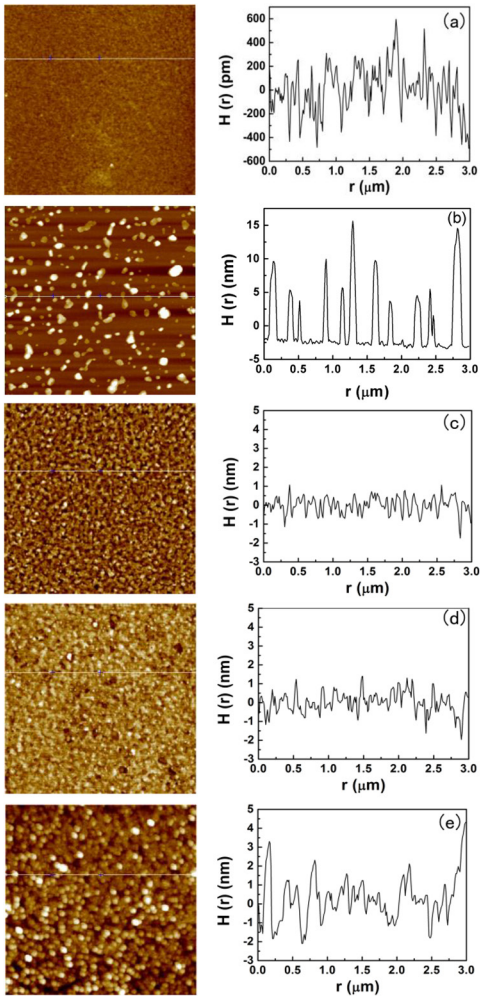

Figure 1. AFM images (3 μm × 3 μm) and 1D cross section scan of (a) Si surface, and $MAPbI_3$ thin film for deposition time of (b) 130, (c) 200, (d) 300 and (e) 600 s.

initial growth when the atoms of film are more strongly coupled with each other than with the substrate [14], and a similar Volmer–Weber growth of $MAPbI_3$ films has been demonstrated during the hot casting process [9].

In figure 2(a) we plot $H(r, t) - r$ curve in log–log scale for the films on Si substrates. At small lateral length ($r \ll \xi$), height–height correlation function do not overlap with each other, this implies that the growth is not stationary, i.e. the local slope is a function of growth time [15].

In this short length scale, linear relationship between $H(r, t)$ and r is observed. By the liner fitting of this part, α can be obtained (listed in table 1). For the initial film growth before formation of continuous film ($t < 200$ s), α exhibits a significantly change as shown in figure 2(c), indicates strong interaction between the incoming flux and the substrates for initial coverage. During this stage the surface experiences unstable scaling behavior [16]; in the second stage ($t \geqslant 200$ s), α almost invariant and average α value about 0.70 is yield after the formation of continuous film, indicating a onset of stable scaling behavior [17].

The calculated values of interface width w, and correlation length ξ are listed in table 1. In figure 3 we plot curve of (a) w, and (b) ξ, as a function of growth time t. It shows that at initial growth process, the interface width w and correlation length ξ both decrease with increasing deposition time. As more materials are deposited, the transition of morphology which occurs after continuous film formed is accompanied by increase of w and ξ with the growth time. Figure 3 indicates that the surface evolves from a dynamic smoothening process to roughening growth, which is consistent with the 1D cross-section scans in figure 1. Similar results are also observed in those of other group's work [18, 19].

According to the relationships of $w(t) \propto t^{\beta}$, and $\xi(t) \propto t^{1/z}$, a linear fit of log$w$–log$t$ and logξ–log$t$ plot of continuous film ($t \geqslant 200$ s) results in the following value: $\beta = 0.79 \pm 0.057$, $1/z = 0.78 \pm 0.038$. The value of α and β yields a ratio of $\beta/\alpha \approx 1.13$ and gives $\beta/\alpha = 1/z + 0.35$. This means that the growth behavior is non-stationary and undertakes anomalous growth where the short-range behavior of the height–height correlation function is no longer time independent [13], this supports the result as revealed in figure 2(a).

After the onset of stable scaling behavior ($t \geqslant 200$ s), the average α value ≈0.7 of the $MAPbI_3$ thin films deposited on Si substrates is quite close with those of growth models incorporating surface diffusion or bulk diffusion

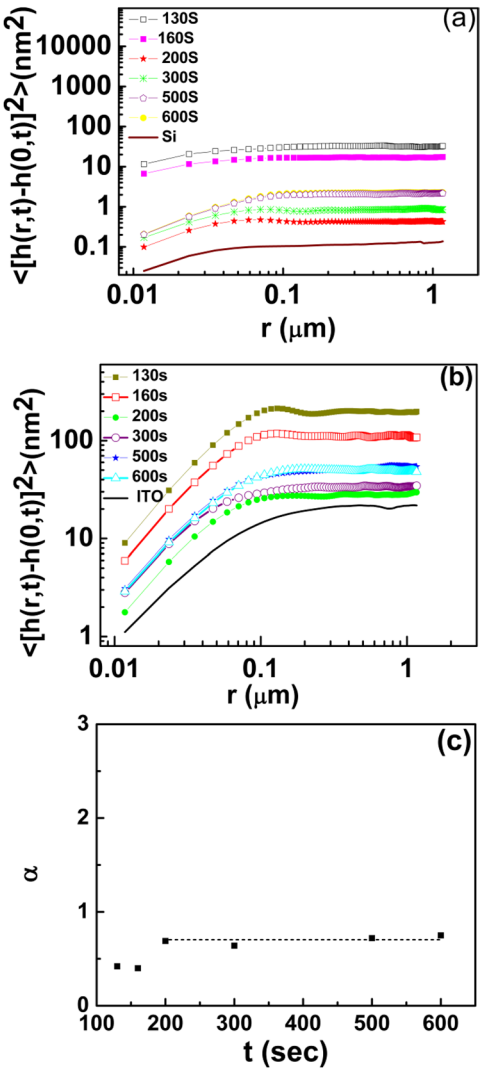

Figure 2. Log $H(r)$ versus Log r curve of $CH_3NH_3PbI_3$ films with different thickness on (a) Si substrates and (b) ITO substrates. (c) Roughness exponent α as a function of growth time t for $MAPbI_3$ thin films on Si substrates, the dotted line shows the average of α when $t \geqslant 200$ s.

Table 1. Surface parameters α, w and ξ for $MAPbI_3$ samples deposited on Si and ITO substrates.

	Time(s)	130	160	200	300	500	600
Si	α	0.42	0.40	0.69	0.64	0. 72	0.75
	$w(t)$ (nm)	4.03	2.89	0.46	0.65	1.01	1.06
	$\xi(t)$ (μm)	0.027	0.025	0.022	0.031	0.047	0.050
ITO	α	0.89	0.88	0.84	0.83	0.83	0.83
	$w(t)$ (nm)	10.02	7.44	3.75	4.08	4.87	5.05
	$\xi(t)$ (μm)	0.058	0.054	0.051	0.054	0.062	0.068

(α is from 0.66 to 1.0) [15, 20–22]. However, $\beta = 0.20$–0.25 derived from processing predominated by surface diffusion or bulk diffusion, is hard to explain the high $\beta \approx 0.80$ in this work. Pervious study revealed that in the case of mound growth, $\beta \geqslant 0.5$ [23, 24]. For mound growth, the local surface is smooth and $\alpha = 1$, but in practices may go down to a lower value, e.g. $SnCl_2Pc$ on glasses ($\alpha = 0.9$), phthalocyanine (H_2Pc) on glasses ($\alpha = 0.61 \pm 0.12$) [25, 26]. There for, possible of mound growth also cannot be excluded.

The β value about 0.80 in this work is considerably higher than those predicted by conventional mound growth [23, 27]. High value of β implies rapid roughening when certain regions of the surface persistently grow faster than others (e.g. Diindenoperylene on Si, $a \approx 0.684$, $\beta \approx 0.748$, $1/z \approx 0.92$) [28], which usually associate with shadowing effect or step-edge barrier (Schwoebel barrier). Extreme high value of $\beta = 1$ has been reported in the simulation result under pure shadowing induced mound growth [29], and $\beta = 1.02$ in [26] is suggested to arise from the pronounced step-edge barrier induced upward growth of mound at initial stages of the thin film growth.

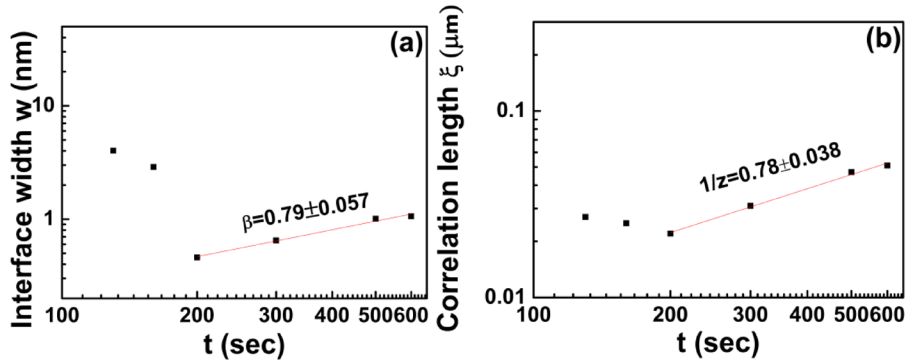

Figure 3. Log–log plot of (a) w, (b) ξ, as a function of growth time t for $MAPbI_3$ thin films on Si substrates, the solid line is a liner fit to the data of growth time $t \geqslant 200$ s, which gives β and $1/z$, respectively.

In order to identify the origin of the roughening in the growth, we have investigated the ring behavior of the $MAPbI_3$ thin films. The ring structure is one main feature of mound growth induced by step-edge barrier (often referred to as an instability) differs from other roughness mechanisms [13]. 2D fast Fourier transform (FFT) of the representative $MAPbI_3$ surface on Si substrates from the AFM images are shown in figures 4(a)–(c). The ring like behavior is obvious for these films. The ring radius enlarged when growth time increases. In this case, the step-edge barrier induced mound growth is the most likely govern mechanism for the film formation process of the $MAPbI_3$ films on Si substrates.

If we neglect the weak effects of non-linearities, the step-edge barrier induced growth model can be described by equation (2) [13]:

$$\left(\frac{\partial h}{\partial t} = -\nu \nabla^2 h - k \nabla^4 h + \eta\right). \tag{2}$$

Where ν terms refers to adatom diffusion process (step-edge barriers effect), and k terms is due to surface diffusion. The term η represents a random fluctuation arising from the deposition. The ratio k/ν plays an important role for growth mechanism. If $k/\nu \gg 1$, indicates that either step-edge barriers is small or surface diffusion is strong and the ring structure can be hardly recognized. As the k/ν ratio decrease, the ring structure is obvious and the ring radius spread out, which means the step-edge barrier dominates the growth of the film. Thus, the larger radius of rings structure indicates a stronger step-edge barrier in the later film growth stage of $MAPbI_3$. This gradual increase of step-edge barrier with thickness as an origin of mound formation has also been observed in other works [24, 30], and this phenomenon is considered to be related to thickness dependent structural changes or molecular reorientation.

The simulation model in [26] gives $\beta = 1.02 \pm 0.08$, in case of mound only growing upward. But this model is restricted to the dynamic exponent taking on $1/z = 0$, where all lateral mass transport behavior between individual mounds is suppressed because of the step-edge barrier. But for $MAPbI_3$ thin films on Si substrates, when $t \geqslant 200$ s, scaling exponents $1/z \approx 0.78$ demonstrates the existence of a lateral mass transport of the molecule between mounds or from top of the island to the substrate, rather than the only upward mound growing. However, upward growth induced by the step-edge barrier we argue for $MAPbI_3$ films on Si substrates is much stronger than the lateral mass transport, and the preferred mound growth gives rise to rapid roughening and ultimately induces scaling behavior with a large global β. The high value of $\beta \approx 0.79$ may be the evidence that step edge barrier induced upward growth is effective in the formation of the rapid surface roughening of these films. Further, large discrepancy of λ value of 0.35 between β/α and $1/z$, and anomalous scaling behavior in the $MAPbI_3$ films on Si substrates also clearly suggests this dominate up growth that corresponds to the roughening mechanism of the film growth as observed [26].

4.2. The substrates effect on the growth behavior of $MAPbI_3$ thin films

Practical applications of devices require the perovskite thin films deposited on a wide variety of substrates. The nucleation and growth of the deposited perovskite thin films performance is strongly dependent on the surface properties of the substrates, duo to the sensitivity of crystallization on interfacial structure [31]. To determine the initial substrate effect on the growth behavior of the $MAPbI_3$ films, $MAPbI_3$ films on ITO substrates are tested as comparison. Table 1 shows the calculated value of α, w and ξ of $MAPbI_3$ films on ITO substrates.

Results show that the interface width w decreases firstly and then increases with the growth of time for the films on ITO substrates, and this is in the same way of those on Si substrates. The ring structures are observed for the initial films for growth time $t < 200$ s both on Si and ITO substrates (figures 4(a) and (d)). However, for

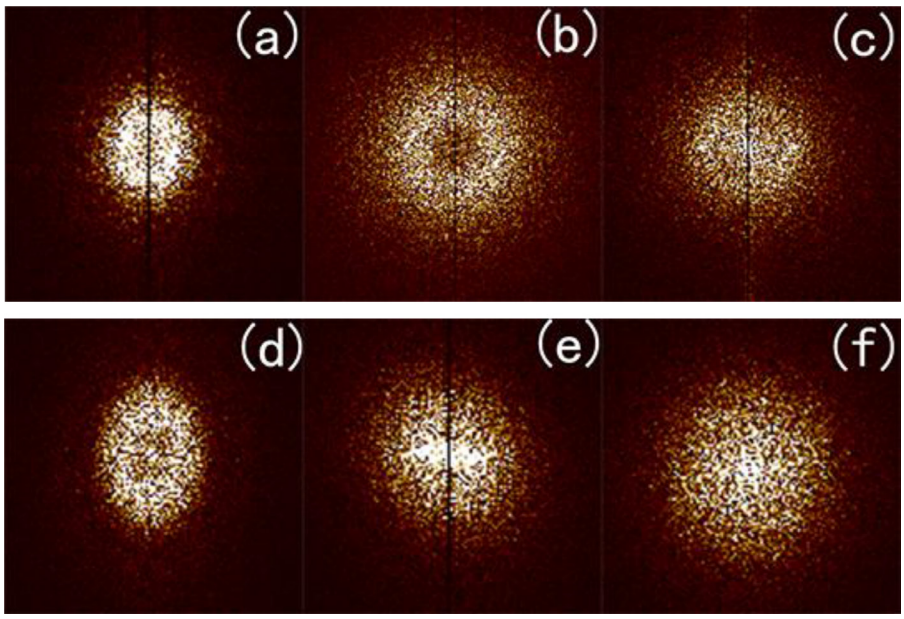

Figure 4. 2D FFT of the surface from $MAPbI_3$ thin film AFM images on Si substrates of growth time (a) 160 s, (b) 200 s and (c) 300 s, and on ITO substrates of growth time (d) 130 s, (e) 200 s and (f) 300 s. The vertical dark line in the center of the image ((a)–(c) and (e)) is duo to the AFM fast scan direction.

$t \geqslant 200$ s, the ring radius shrinks and not be observed for the films on ITO substrates (figures 4(e) and (f)), this is quite different from that of the films deposited on Si substrates. The ring structure shift of $MAPbI_3$ films growth on ITO substrates might indicate the transition of the dominate growth mechanism. According to the situation of $k/\nu \gg 1$ as discussed in equation (2) aforementioned, the step edge barrier effect may be very small for the $MAPbI_3$ films on ITO when $t \geqslant 200$ s. The calculated scaling exponents $\alpha \sim 0.83$, $\beta = 0.28 \pm 0.02$, $1/z = 0.26 \pm 0.04$ and $\beta/\alpha = 1/z + 0.07$ of $MAPbI_3$ deposited on ITO substrates are also different from those of the films on Si substrates. Mullins growth is the govern mechanism of the films growth on ITO substrates for $t \geqslant 200$ s are confirmed (unpublished results). The small $\beta = 0.26 \pm 0.02$ of the films on ITO substrates may be attribute to the weak step edge barrier effect, while higher step-edge barrier give rise to the higher β value of $MAPbI_3$ film on Si.

At small lateral length ($r \ll \xi$), height–height correlation functions do not overlap with each other for the films on ITO substrates (figure 2(b)), suggesting the similar non-stationary films growth behavior with that on Si substrates. However, the rate of change of the local slope with time on Si substrates has relatively strong time dependence in comparison with that on ITO substrates. This is consistent with non-local effect induced interface instability where high β value exists [32]. Further, this is supported by the much larger λ value of 0.35 of $MAPbI_3$ films on Si substrate than that of 0.07 on ITO, implying more significant anomalous scaling behavior on Si substrates than on ITO ones.

These results show that the growth behavior of $MAPbI_3$ thin films is affected considerably by the substrates which thin films is deposited onto. The films growth behavior dependence on the substrates have been investigated in many reports for better understanding the growth mechanism of thin films, e.g. $F_{16}CoPc$ thin films show larger β value of 0.56 on SiO_2 than those of 0.32 on organic DIP substrates [30]; the substrates effect induced difference of scaling behavior of perylene thin films on glass ($\alpha \approx 0.82$, $\beta \approx 0.21$) and Au substrates ($\alpha \approx 0.84$, $\beta \approx 0.74$) [16]; and very recent report of vacuum-deposited $SnCl_2Pc$ organic films, where β is found to be much larger for film on glass substrates (0.48) than on Si (1 0 0) (0.21) substrates [25]. The influence of substrates can be attributed to substrates morphology, lattice mismatch, interaction of molecules with the substrates, etc, and all that factors could give rise to different growth effect, such as different molecular structures, grain shape and initial nucleation density [13, 25, 30]. Different substrate induced various ratios of step-edge barrier and surface diffusion before and after the formation of continuous films, might lead to structural changes or molecular reorientation of $MAPbI_3$ thin films [24, 30], is considered to be a possible reason for the substrate-dependent growth behavior of $MAPbI_3$ thin films as revealed in our work. The growth behavior of $MAPbI_3$ thin films is believed strongly depends on initial surface configurations and other deposition conditions.

5. Conclusions

We address the morphology evolution and growth dynamics of $MAPbI_3$ perovskite thin films grown by thermal evaporation. The anomalous scaling behavior of the $MAPbI_3$ films on Si substrates is observed. After the growth time $t \geqslant 200$ s, the formation of continuous films and stable scaling occur, and scaling exponent $\alpha \sim 0.70$, growth

exponent $\beta = 0.79 \pm 0.057$, dynamic exponents $1/z = 0.78 \pm 0.038$ is obtained. 2D fast Fourier transform analysis reveals that mound growth induced by step-edge barrier may play the dominate role in the growth mechanism for the film on Si substrates. $\alpha \sim 0.83$, and much smaller value of $\beta = 0.28 \pm 0.02$, $1/z = 0.26 \pm 0.04$, and different ring's behavior of $MAPbI_3$ films deposited on ITO substrates is also presented for comparison, which exhibits different growth behavior of $MAPbI_3$ films from those on Si substrates, suggesting a crucial important effect of the film-substrates interface properties on the growth mechanism of $MAPbI_3$ perovskite thin films.

Acknowledgment

The financial support of the National Natural Science Foundation of China (11404191, 61604149, and 61604089), and Shandong Provincial Natural Science Foundation (ZR2016FB16, ZR2015FQ004, ZR2016AQ14) is fully acknowledged. We would also like to acknowledge the support of Program for the Top Young of SDUT, People's Republic of China.

References

[1] Liu M, Johnston M B and Snaith H J 2013 *Nature* **501** 395
[2] Dou L T, Yang Y M, You J B, Hong Z R, Chang W H, Li G and Yang Y 2014 *Nat. Commun.* **5** 5404
[3] Deschler F *et al* 2014 *J. Phys. Chem. Lett.* **5** 1421
[4] Tan Z-K *et al* 2014 *Nat. Nanotechnol.* **9** 687
[5] Kojima A, Teshima K, Shirai Y and Miyasaka T 2009 *J. Am. Chem. Soc.* **131** 6050
[6] Research cell efficiency records www.nrel.gov/ncpv Accessed 1 April 2016 National Renewable Energy Laboratory
[7] Jeon N J *et al* 2015 *J. Phys. Chem. Lett.* **6** 129
[8] Nam J J, Jun H N, Young C K, Woon S Y, Seung C R and Sang S II 2014 *Nat. Mater.* **13** 897
[9] Zheng Y C, Yang S, Chen X, Chen Y, Hou Y and Yang H G 2015 *Chem. Mater.* **27** 5116
[10] Rajamanickam N, Kumari S, Vendra V K, Lavery B W, Spurgeon J, Druffel T and Sunkara M K 2016 *Nanotechnology* **27** 235404
[11] Chen C W, Kang H W, Hsiao S Y, Yang P F, Chiang K M and Lin H W 2014 *Adv. Mater.* **26** 6647
[12] Gedda M, Subbarao N V V and Goswami D K 2014 *Langmuir* **30** 8735
[13] Zhao Y P, Wang G C and Lu T M 2001 *Characterization of Amorphous and Crystalline Rough Rurface: Principles and Applications* (New York: Academic)
[14] Raoufi D and Hosseinpanahi F 2013 *J. Theor. Appl. Phys.* **7** 1
[15] Zhao Y P, Fortin J B, Bonvallet G, Wang G C and Lu T M 2000 *Phys. Rev. Lett.* **85** 3229
[16] Zorba S, Yan L, Watkins N J and Gao Y 2002 *Appl. Phys. Lett.* **81** 5195
[17] Yang J J, Tang J, Liu N, Ma F, Tang W and Xu K W 2012 *J. Appl. Phys.* **111** 104303
[18] Ballestad A, Ruck B J, Adamcyk M, Pinnington T and Tiedje T 2001 *Phys. Rev. Lett.* **86** 2377
[19] Liu Z J, Shum P W and Shen Y G 2005 *Appl. Phys. Lett.* **86** 251908
[20] Kardar M, Parisi G and Zhang Y C 1986 *Appl. Phys. Lett.* **56** 889
[21] Lai Z W and Das S S 1991 *Phys. Rev. Lett.* **66** 2348
[22] Yang J J, Miao F M, Tang J, Yang Y Y, Liao J L and Liu N 2014 *Thin Solid Films* **550** 367
[23] Ernst H, Fabre F, Folkerts R and Lapujoulade J 1994 *Phys. Rev. Lett.* **72** 112
[24] Hlawacek G, Puschnig P, Frank P, Winkler A, Ambrosch-Draxl C and Teichert C 2008 *Science* **321** 108
[25] Obaidulla S M and Giri P K 2015 *Appl. Phys. Lett.* **107** 221910
[26] Yim S and Jones T S 2006 *Phys. Rev.* B **73** 161305
[27] Barabási A L and Stanley H E 1995 *Fractal Concepts in Surface Growth* (Cambridge: Cambridge University Press)
[28] Dürr A C, Schreiber F, Ritley K A, Kruppa V, Krug J, Dosch H and Struth B 2003 *Phys. Rev. Lett.* **90** 016104
[29] Pelliccione M, Karabacak T and Lu T M 2006 *Phys. Rev. Lett.* **96** 146105
[30] Zhang Y, Barrena E, Zhang X N, Turak A, Maye F and Dosch H 2010 *J. Phys. Chem.* C **114** 13752
[31] Docampo P, Ball J M, Darwich M, Eperon G E and Snaith H J 2013 *Nat. Commun.* **4** 657
[32] Vázquez L, Albella J M, Salvarezza R C, Arvia A J, Levy R A and Perese D 1996 *Appl. Phys. Lett.* **68** 1285